

## 一维链状配位聚合物 $[\text{Cu}(\text{H}_2\text{btc})(\text{H}_2\text{O})_3] \cdot 3\text{H}_2\text{O}$ 的非等温反应动力学和晶体结构

郭金玉 张同来\* 张建国 乔小晶 杨 利 于 伟 吴瑞凤  
(北京理工大学爆炸科学与技术国家重点实验室, 北京 100081)

**摘要:** 为研究配位聚合物 $[\text{Cu}(\text{H}_2\text{btc})(\text{H}_2\text{O})_3] \cdot 3\text{H}_2\text{O}$  ( $\text{H}_2\text{btc}=1,2,4,5\text{-benzenetetracarboxylate}$ ) 的热分解机理和非等温反应动力学进行了 DSC 和 TG-DTG 热分析。由热分析结果和 FTIR 光谱推测了其热分解机理; 将 Kissinger 法、Ozawa 法、积分法和微分法得到的动力学参数进行比较确定了第一个失重过程最可能的动力学模型函数。配位聚合物的 X 射线单晶结构分析表明它由 $[\text{Cu}(\text{H}_2\text{btc})(\text{H}_2\text{O})_3]_n$  分子链组成, 并有客体水分子通过分子间氢键附着在分子链上。这一结构特点与热分析结果相一致。还有一种氢键将分子链连接起来形成二维框架, 这一框架在失去配位水和结晶水后到 553 K 开始分解。

**关键词:** 热分解机理; 非等温反应动力学; 均苯四甲酸; 一维框架结构

中图分类号: O614.121; O641; O642

文献标识码: A

文章编号: 1001-4861(2006)06-2179-07

## Non-isothermal Kinetics and Crystal Structure of One-dimensional Coordination Polymer $[\text{Cu}(\text{H}_2\text{btc})(\text{H}_2\text{O})_3] \cdot 3\text{H}_2\text{O}$

GUO Jin-Yu ZHANG Tong-Lai\* ZHANG Jian-Guo QIAO Xiao-Jing YANG Li YU Wei WU Rui-Feng  
(State Key Laboratory of Explosion Science and Technology, Beijing Institute of Technology, Beijing 100081)

**Abstract:** Thermal analyses DSC and TG-DTG have been performed on the title coordination polymer ( $\text{H}_2\text{btc}=1,2,4,5\text{-benzenetetracarboxylate}$ ) to investigate its thermal decomposition mechanism and the associated kinetics. The thermal decomposition mechanism is predicted based on DSC, TG-DTG and FTIR techniques. The most probable kinetic model function of the first mass loss stage is determined by comparison of kinetic parameters obtained by using Kissinger, Ozawa, integral and differential methods. The coordination polymer is comprised of the molecular chains of  $[\text{Cu}(\text{H}_2\text{btc})(\text{H}_2\text{O})_3]_n$  with guest water molecules linked by intermolecular hydrogen bonds. This structural feature is in agreement with the results of the thermal analyses on the coordination polymer. Another kind of hydrogen bonds that link the molecular chains together to form the two-dimensional frameworks make the molecules stable up to 553 K after the release of the coordination and lattice waters. CCDC: 611873.

**Key words:** thermal decomposition; non-isothermal kinetics; 1,2,4,5-benzenetetracarboxylic acid; one-dimensional framework

## 0 Introduction

In the past few decades, aryl carboxylic acids have attracted much attention in the preparation of the

coordination polymers with novel structures<sup>[1-9]</sup>. The coordination polymers using aryl carboxylic acids as ligands possess novel microporous rigid frameworks and suggest potential uses in fields such as optical materia-

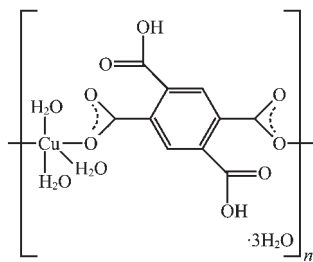
收稿日期: 2006-07-04。收修改稿日期: 2006-09-14。

国家自然科学基金资助项目(No.20471008)和北京理工大学基础研究基金资助项目(No.BIT-UBF-200502B4221)。

\*通讯联系人。E-mail: ztlbit@bit.edu.cn

第一作者: 郭金玉, 男, 26 岁, 博士研究生; 研究方向: 含能配合物。

ls<sup>[10–15]</sup>, magnetic materials<sup>[16–20]</sup> and gas storages<sup>[21–24]</sup>. Of the aryl carboxylic acids, 1,2,4,5-benzenetetracarboxylic acid has less been studied<sup>[25]</sup>. In this paper,  $\{[\text{Cu}(\text{H}_2\text{btc})(\text{H}_2\text{O})_3] \cdot 3\text{H}_2\text{O}\}_n$  (polymer **1**) has been synthesized using 1,2,4,5-benzenetetracarboxylic acid as ligand by hydrothermal method. In order to investigate its thermal properties, thermal analyses DSC and TG-DTG have been performed on the polymer to predict its thermal decomposition mechanism and to determine its non-isothermal kinetic model function of the first mass loss stage. X-ray single crystal structure analysis demonstrates the crystal structure of the polymer as the coordination pattern schemed as follows.



Scheme for connection mode of polymer **1**

The crystal pattern is corresponding to the results of the thermal analyses.

## 1 Experimental

### 1.1 Instruments and synthesis

Elemental analysis was carried on Flash EA 1112 full-automatic micro-analyzer. FTIR spectra were recorded on Bruker Equinox 55 infrared spectrometer using KBr pellet in the range of 4 000~400  $\text{cm}^{-1}$  with the resolution of 4  $\text{cm}^{-1}$ . Pyris 1 Differential Scanning Calorimeter (Perkin Elmer, U.S.A.) and Pyris 1 Thermogravimetric Analyser (Perkin Elmer, U.S.A.) were used to perform thermal analyses in a flowing  $\text{N}_2$  gas rate of 20  $\text{mL} \cdot \text{min}^{-1}$ . The conditions for the thermal analyses are: for Pyris 1 DSC, the crystal sample was powdered and sealed in aluminum pan, the heating rates are 2, 5, 10, 15, 20, 25  $\text{K} \cdot \text{min}^{-1}$ ; for Pyris 1 TGA, the crystal sample was powdered and put in the platinum sample pan, the heating rate is 10  $\text{K} \cdot \text{min}^{-1}$ .

1,2,4,5-Benzenetetracarboxylic acid (BTCA, A. R.),  $\text{Cu}(\text{NO}_3)_2 \cdot 3\text{H}_2\text{O}$  (A.R.), DMF (A.R.), pyridine (A.

R.). All the reagents are bought from the Reagents Company and not further purified. A mixture of  $\text{Cu}(\text{NO}_3)_2 \cdot 3\text{H}_2\text{O}$  0.241 6 g (1 mmol), 1,2,4,5-benzenetetracarboxylic acid 0.254 1 g (1 mmol) and 4,4'-bipyridine was dissolved in 6 mL DMF. 5% NaOH and 5%  $\text{HNO}_3$  solutions were used to adjust the pH value to about 6~7. Then the above system was transferred to 25 mL Teflon-lined stainless-steel container. The container was controlled by a programmed temperature as follows: from room temperature to 373 K, 0.5  $\text{K} \cdot \text{min}^{-1}$ ; 373 K for 48 h; 373 K to 393 K, 0.5  $\text{K} \cdot \text{min}^{-1}$ ; 393 K for 24 h; from 393 K to room temperature automatically. Crystals suitable for X-ray single crystal diffraction were collected by filtration, separated and washed with DMF (4 mL  $\times$  2), then dried in vacuum. Yield about 83% based on Cu. Anal. for  $\text{C}_{10}\text{H}_{16}\text{CuO}_{14}$  Calcd. (wt%): C, 28.34; H, 3.81. Found (wt%): C, 28.45; H, 3.76. FTIR (KBr pellet) spectra ( $\text{cm}^{-1}$ ): 3 439 br,s ( $\nu_{\text{O-H}}$ ), 1 675vs ( $\nu_{\text{C=O}}$ ), 1 596vs ( $\nu_{\text{C=O}}$ ), 1 380vs ( $\nu_{\text{C=O}}$ ), 845w ( $\delta_{\text{C-H}}$ ), 695w ( $\delta_{\text{C=O}}$ ).

### 1.2 Crystal structure determination

A block-shaped deep blue crystal with dimensions of 0.26 mm  $\times$  0.22 mm  $\times$  0.18 mm was selected for the structural analysis. Data collection was carried out on Bruker SMART 1000 CCD area detector X-ray single crystal diffractometer using mono-chromatized Mo  $K\alpha$  radiation ( $\lambda=0.071\ 073$  nm) and  $\varphi/\omega$  scanning mode at 294(2) K. Reflections of 2 934 collected in the  $\theta$  range of 2.64~26.34 were used to determine the cell parameters and orientation matrix. The  $\theta$  range for data collection is  $1.86^\circ \leq \theta \leq 26.38^\circ$  and the limiting indices are  $-8 \leq h \leq 8$ ,  $-13 \leq k \leq 11$ ,  $-13 \leq l \leq 12$ . Reflections of 4 418 were collected, of which 2 649 are unique, 2 514 with  $I > 2\sigma(I)$  were considered as observed. The structure was solved by direct methods using SHELXS-97 program<sup>[26]</sup> and refined by full-matrix least squares on  $F^2$  using SHELXL-97 program<sup>[27]</sup>. Some of the non-hydrogen atoms were obtained from the difference Fourier map, and all the non-hydrogen atoms were refined anisotropically. The hydrogen atoms were obtained geometrically and constrained in the locations during refinements. The crystallographic data are listed in Table 1.

CCDC: 611873.

**Table 1 Detailed crystallographic data of polymer 1**

Empirical formula	C <sub>10</sub> H <sub>16</sub> CuO <sub>14</sub>	Reflections collected	4 418
Formula weight	423.77	Independent reflections	2 649 ( $R_{\text{int}}=0.025\ 3$ )
Crystal system	Monoclinic	Data / restraints / parameters	2 649 / 22 / 226
Space group	<i>Pn</i>	$F(000)$	434
$a / \text{nm}$	0.676 4(1)	$V / \text{nm}^3$	0.802 5(2)
$b / \text{nm}$	1.093 4(2)	$Z$	2
$c / \text{nm}$	1.085 7(2)	$D_c / (\text{g} \cdot \text{cm}^{-3})$	1.754
$\beta / (^\circ)$	91.93(3)	$R$ indices for all data	$R_1=0.036\ 2$ , $wR_2=0.089\ 2$
$\theta$ range for data collection / ( $^\circ$ )	1.86~26.38	Final $R$ indices [ $I>2\sigma(I)$ ]	$R_1=0.033\ 4$ , $wR_2=0.086\ 7$
Indices range ( $h, k, l$ )	$-8 \leq h \leq 8, -13 \leq k \leq 11, -13 \leq l \leq 12$	$S$	1.049
$\mu(\text{Mo K}\alpha) / \text{mm}^{-1}$	1.436	Largest difference peak and hole / ( $\text{e} \cdot \text{nm}^{-3}$ )	232 and -290

$$^a w=1/[s^2(F_o^2) + (0.051\ 5P)^2 + 0.647\ 6P] \text{ where } P=(F_o^2 + 2F_c^2)/3.$$

## 2 Results and discussion

### 2.1 Thermal analyses

In the DSC curve of polymer **1** at a heating rate of  $10\ \text{K} \cdot \text{min}^{-1}$  (Fig.1), there are one endothermic (peak temperature 384 K) and one exothermic (peak temperature 592 K) processes. The peak temperatures and the related kinetic parameters of the endothermic process at different heating rates are listed in Table 2<sup>[28,29]</sup>. The details of both heat effects will be discussed

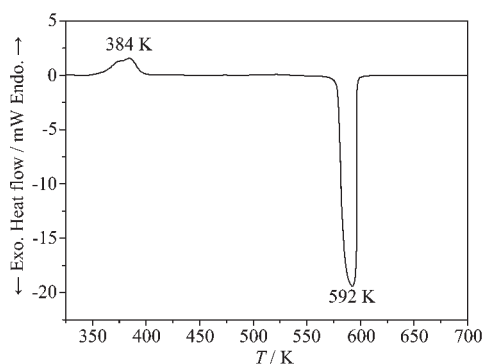


Fig.1 DSC curve of polymer **1** in a flowing  $\text{N}_2$  gas and at a heating rate of  $10\ \text{K} \cdot \text{min}^{-1}$

in the following TG-DTG analysis.

The TG-DTG curves (Fig.2) demonstrate that there are three main mass loss stages: from 344 to 453 K, 24.80%; from 453 to 553 K, 22.05%; from 553 to 593 K, 38.58%. The first stage is predicted as the loss of the six water molecules (Calcd. 25.51%)-three lattice and three coordination water molecules. The loss of the water molecules from polymer **1** can be demonstrated by the missing of the vibrations of the water at  $3\ 439\ \text{cm}^{-1}$ . This stage is corresponding to the endothermic process in the DSC curve. The second mass loss stage is slow and predicted as the loss of the two uncoordinated carboxylic groups (Calcd. 21.24%). There is no distinguishing heat effect during this mass loss stage in the DSC curve. The third mass loss stage is intense and assigned to be the decomposition of the polymer with final residue 15.66%. There is an obvious and intense exothermic peak in the DSC curve in relation to this mass loss stage. The composition of the final residue is

**Table 2 Calculated kinetic parameters for the first mass loss stage of polymer 1 determined from the DSC curves at various heating rates**

$\beta / (\text{K} \cdot \text{min}^{-1})$	$T_c / \text{K}$	$T_p / \text{K}$	$E_K / (\text{kJ} \cdot \text{mol}^{-1})$	$-r_K$	$\lg A_K / \text{s}^{-1}$	$E_O / (\text{kJ} \cdot \text{mol}^{-1})$	$-r_O$
2	355.25	375.45	135.00	0.9737	16.49	134.50	0.9760
5	358.55	380.25					
10	360.65	384.75					
15	362.95	388.95					
20	366.45	393.65					
25	368.65	397.05					
Mean $E_a$			134.75				

$T_c$ : onset temperature in the DSC curve;  $T_p$ : maximum peak temperature; Subscript K: Kissinger's method; O: Ozawa's method.

predicted based on the FTIR spectra of the residues got at 593 K. The vibrations at 730 and 500  $\text{cm}^{-1}$  demonstrate the formation of CuO (Calcd. 18.77%)<sup>[30]</sup>.

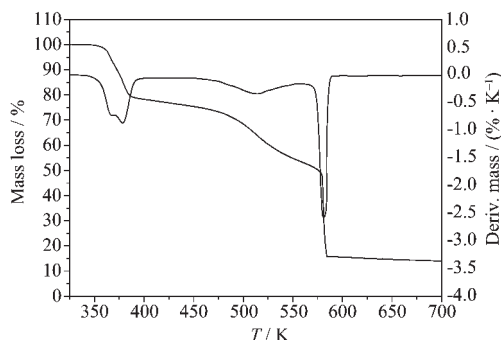


Fig.2 TG-DTG curve of polymer 1 in a flowing  $\text{N}_2$  gas and at a heating rate of  $10 \text{ K} \cdot \text{min}^{-1}$

Using the single non-isothermal DTG curve got under the flowing  $\text{N}_2$  gas with the heating rate of  $10 \text{ K} \cdot \text{min}^{-1}$ , the values of  $E_a$ ,  $A$  and the most probable kinetic model function of the first mass loss from the coordination polymer were obtained with integral equations (Eqs.(1)~(3)) and differential equation (Eq. (4))<sup>[31~34]</sup>. The detailed data used for the integral equations (Eqs. (1)~(3)) and differential equation (Eq. (4)) are listed in Table 3.

Table 3 Basic data for the first mass loss stage of polymer 1

Data point	$T_0=339.69 \text{ K}; \beta=10 \text{ K} \cdot \text{min}^{-1}$		
	$T_i / \text{K}$	$\alpha_i$	$(d\alpha/dt)_i \times 10^4 / \text{s}^{-1}$
1	341.69	0.000 1	0.666 7
2	345.69	0.001 7	1.529 9
3	349.69	0.007 3	4.038 5
4	353.69	0.020 6	8.931 6
5	357.69	0.049 1	19.660 0
6	361.69	0.112 6	37.210 0
7	365.69	0.226 1	53.910 0
8	369.69	0.364 1	61.350 0
9	373.69	0.509 6	64.890 0
10	377.69	0.667 8	66.510 0
11	381.69	0.824 8	56.200 0
12	385.69	0.931 9	33.820 0
13	389.69	0.981 5	13.120 0
14	393.69	0.995 2	3.617 9
15	397.69	0.999 0	1.166 7
16	399.69	0.999 8	0.666 7

$T_0$ : the initial point at which DTG curve deviates from the baseline;  $\beta$ : the heating rate.

Integral method:

MacCallum-Tanner Method:

$$\lg[G(\alpha)] = \lg \frac{AE_a}{\beta R} - 0.4828 E_a^{0.4357} - \frac{0.449 + 0.217 E_a}{0.001} \frac{1}{T} \quad (1)$$

Satava-Sestak Method:

$$\lg[G(\alpha)] = \lg \frac{AE_a}{\beta R} - 2.315 - 0.4567 \frac{E_a}{RT} \quad (2)$$

General and Agrawal Method:

$$\ln \left[ \frac{G(\alpha)}{T^2} \right] = \ln \left[ \frac{AR}{\beta E_a} \frac{1 - 2(RT/E_a)}{1 - 5(RT/E_a)^2} \right] - \frac{E_a}{RT} \quad (3)$$

Differential method:

Achar, Brindley and Sharp Equation:

$$\ln \left[ \frac{d\alpha}{f(\alpha)dt} \right] = \ln A - \frac{E_a}{RT} \quad (4)$$

where  $f(\alpha)$  and  $G(\alpha)$  are the differential and integral model functions, respectively,  $R$  is the gas constant,  $\alpha$  is the conversion degree ( $\alpha = H_t/H_0$ ),  $H_0$  is the total heat effect corresponding to the global area under the DTG curve,  $H_t$  is the reaction heat at a certain time (corresponding to the partial area under the DTG curve),  $T$  is the temperature at time  $t$ ,  $\beta$  is the heating rate.

Thirty-six types of kinetic model functions and the data in Table 3 are put into Eqs. (1)~(4) for calculations. The probable kinetic model function is determined based on  $E_a$  and  $\lg A$  whose values are very close to each other with the better values of  $r$ ,  $Q$  (stand mean square deviation) and  $d$  (believable factor,  $d = Q(1-r)$ ) by comparison. The values of  $E_a$ ,  $A$ ,  $r$ ,  $Q$  and  $d$  are obtained by the linear least squares and iterative methods. For the first mass loss of the six water molecules, the reaction mechanism of the process is classified as nucleation and growth and the mechanism function is the Avrami-Erofeev (with  $n=1$ ) equation<sup>[35]</sup>. The calculated values of the kinetic parameters of the first mass loss stage and its probable kinetic model function are listed in Table 4. Substituting  $f(\alpha)$ ,  $E_a$  and  $A$  with the obtained data in Eq.(5), the kinetic equation of the first mass loss stage is established in Eq.(6).

$$\frac{d\alpha}{dt} = \frac{A}{\beta} f(\alpha) \exp\left(-\frac{E_a}{RT}\right) \quad (5)$$

Table 4 Calculated kinetic parameters of the first mass loss stage of polymer 1

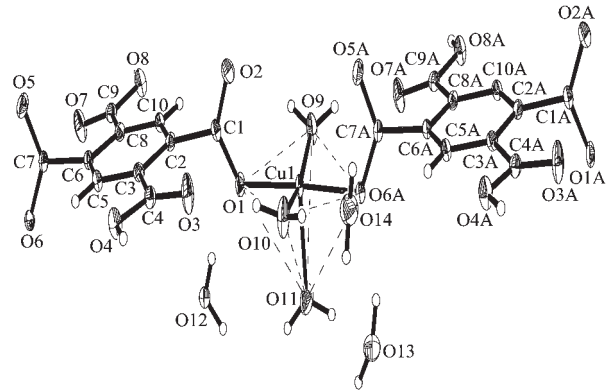
Equation number	Model function	$E_a$ / (kJ·mol <sup>-1</sup> )	lg(A / s <sup>-1</sup> )	-r	Q	d
Eq.(1)	16	165.5	21.11	0.979 7	0.276 8	0.548 0
Eq.(2)	16	164.4	21.03	0.979 7	0.276 8	0.548 0
Eq.(3)	16	166.7	24.88	0.978 7	0.639 7	1.265 4
Eq.(4)	16	121.5	18.93	0.947 4	0.321 2	0.625 5
Mean		154.5	21.49			

Kinetic equation of the first mass loss stage:

$$\frac{d\alpha}{dT} = \frac{10^{21.49}}{\beta} (1-\alpha)e^{-1.858 \times 10^4 / T} \quad (6)$$

2.2 Crystal structure

Thermal properties are relevant to the crystal structure of polymer **1**. The molecular structure of polymer **1** is illustrated in Fig.3. The Cu (II) center which adopts  $sp^3d^2$  hybridization is coordinated by five oxygen atoms to form a lightly distorted coordination pentahedron. The distortion of the pentahedron can be demonstrated by the bond distances and bond angles related to the Cu center (Table 5), especially the bond angles of O1-Cu1-O6A (176.65(18)°) and O9-Cu1-O10 (164.10(2)°). The two carboxylic groups of one 1,2,4,5-benzenetetracarboxylic acid were deprotonated to monodentately coordinate to two different Cu centers. In each of the smallest asymmetric units, the Cu coordination center is surrounded by three lattice water molecules those linked by intermolecular hydrogen bonds.



The dash lines indicate the pentahedron of the Cu(II) coordination center

Fig.3 Molecular structure of polymer **1** with 30% ellipsoid

In Fig.3, O1, O9, O6A and O10 make up of the bottom of the pentahedron of the Cu center with the plane equation of  $3.313x - 0.742y + 9.252z = 3.8540$ . The distances of the Cu center and vertex O11 atom from the bottom plane are +0.010 8 nm and +0.233 6 nm. Because of the steric hindrance effect, the

Table 5 Selected bond distances (nm) and bond angles (°) for polymer 1

Cu1-O1	0.193 8(2)	O3-C4	0.121 3(5)	C2-C3	0.140 5(5)
Cu1-O6A	0.194 8(3)	O4-C4	0.131 3(5)	C3-C5	0.139 1(5)
Cu1-O9	0.200 2(4)	O5-C7	0.122 7(5)	C5-C6	0.138 9(6)
Cu1-O10	0.196 7(4)	O6-C7	0.127 4(5)	C6-C8	0.139 4(5)
Cu1-O11	0.223 3(4)	O7-C9	0.120 8(5)	C8-C10	0.139 3(5)
O1-C1	0.128 4(5)	O8-C9	0.130 8(5)	C2-C10	0.139 0(5)
O2-C1	0.122 3(5)				
O1-Cu1-O6A	176.65(18)	O6A-Cu1-O11	85.20(1)	C5-C6-C8	119.30(3)
O9-Cu1-O10	164.10(20)	O9-Cu1-O11	99.60(2)	C6-C8-C10	120.40(3)
O1-Cu1-O9	89.82(16)	O10-Cu1-O11	96.30(2)	C2-C10-C8	120.40(3)
O1-Cu1-O10	88.57(18)	O1-C1-O2	125.30(4)	O3-C4-O4	123.10(4)
O1-Cu1-O11	91.49(15)	C3-C2-C10	119.40(3)	O5-C7-O6	124.20(4)
O6A-Cu1-O9	90.43(15)	C2-C3-C5	119.80(3)	O7-C9-O8	123.50(4)
O6A-Cu1-O10	92.10(17)	C3-C5-C6	120.80(3)		

Symmetry transformations used to generate equivalent atoms: A: x, y+1, z.

coordinated carboxylates greatly deviate from the benzene ring plane, compared with the other two unprotonated and uncoordinated carboxylic groups. The dihedral angles of four carboxylates (carboxylic groups) with the benzene ring plane are  $3.0^\circ$  (for O3-C4-O4),  $7.2^\circ$  (for O7-C9-O8),  $85.3^\circ$  (for O5-C7-O6) and  $92.8^\circ$  (for O1-C1-O2) respectively. The little differences on the coordination environments between O1-C1-O2 and O5-C7-O6 carboxylates can be demonstrated by the distances of O2-Cu1 (0.305 3 nm) and O5A-Cu1 (0.288 7 nm), angles of O1-C1-O2 ( $125.32^\circ$ ) and O5A-C7A-O6A ( $124.16^\circ$ ).

Based on the coordination styles of 1,2,4,5-benzenetetracarboxylic acids (Fig.3), the coordinated pentahedra of Cu centers are joined together to form the one-dimensional coordination chain (Fig.4). There exist one kind of intramolecular hydrogen bonds and two kinds of intermolecular hydrogen bonds (Table 6). By means of the intermolecular hydrogen bonds such as O11-H11A...O2 and O11-H11B...O5, the molecular chains are linked together to form the two-dimensional frameworks (Fig.5). By means of another

kind of intermolecular hydrogen bonds, the lattice water molecules are linked in the frameworks to occupy the space among the two-dimensional frameworks.

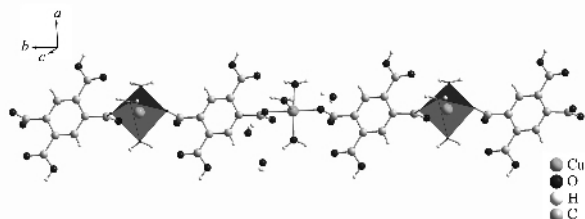


Fig.4 One-dimensional molecular chain of coordination polymer **1** along *b* axis

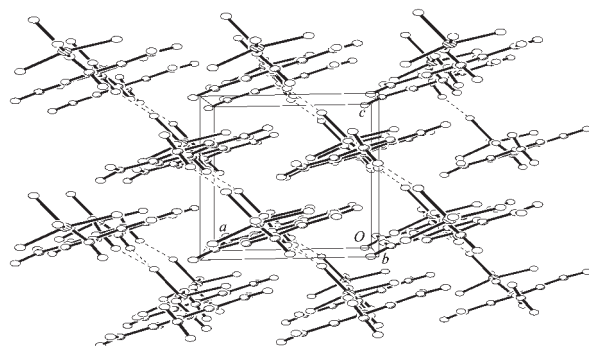


Fig.5 Packing diagram of polymer **1** along *b* axis at the level of 50%

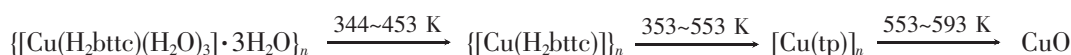
Table 6 Hydrogen bonds existing in the polymer **1**

D-H...A	<i>d</i> (D-H) / nm	<i>d</i> (H...A) / nm	∠DHA / (°)	<i>d</i> (D...A) / nm	Symmetry operations
O4-H4A...O12	0.085 0	0.178 5	176.76	0.263 5	$x-1, y, z$
O8-H8A...O12	0.084 7	0.178 8	171.46	0.262 8	$x+1/2, -y, z-1/2$
O9-H9A...O7	0.085 1	0.211 3	157.42	0.291 8	$x, y+1, z$
O9-H9B...O13	0.085 1	0.190 9	160.36	0.272 5	$x+1/2, -y+1, z-1/2$
O10-H10A...O3	0.085 2	0.208 0	169.54	0.292 2	
O10-H10B...O14	0.085 2	0.185 8	172.45	0.270 5	
O11-H11A...O2	0.085 3	0.206 6	164.56	0.289 7	$x+1/2, -y+1, z+1/2$
O11-H11B...O5	0.085 1	0.196 8	152.55	0.275 2	$x+1/2, -y, z+1/2$
O12-H12A...O5	0.084 8	0.183 8	174.44	0.268 3	$x+1/2, -y, z+1/2$
O12-H12B...O1	0.084 8	0.187 5	165.28	0.270 4	
O13-H13A...O6	0.086 1	0.217 5	156.76	0.298 5	$x, y+1, z$
O13-H13B...O2	0.098 3	0.255 7	118.35	0.314 5	$x+1/2, -y+1, z+1/2$
O13-H13B...O3	0.098 3	0.257 6	112.56	0.308 9	$x+1/2, -y+1, z+1/2$
O14-H14A...O2	0.085 1	0.206 1	165.99	0.289 4	$x-1/2, -y+1, z+1/2$
O14-H14B...O7	0.085 2	0.218 9	157.99	0.299 6	$x-1, y+1, z$

### 3 Conclusions

Based on thermal analyses DSC, TG-DTG and

FTIR spectra, the thermal decomposition mechanism is predicted as follows:





And using Kissinger, Ozawa, integral and differential methods, the kinetic equation of the first mass loss stage is determined as follows:

$$\frac{d\alpha}{dT} = \frac{10^{21.49}}{\beta} (1-\alpha)e^{-1.858 \times 10^4/T}$$

The thermal decomposition mechanism is in good agreement with the crystal structure. The coordination polymer is comprised of the  $[\text{Cu}(\text{H}_2\text{btc})(\text{H}_2\text{O})_3]_n$  molecular chains with guest water molecules linked by intermolecular hydrogen bonds.

## References:

- [1] Sun D F, Cao R, Liang Y C, et al. *J. Chem. Soc., Dalton Trans.*, **2001**:2335~2340
- [2] Li H L, Eddaoudi M, O'Keeffe M, et al. *Nature*, **1999**,**402**: 276~279
- [3] Thirumurugan A, Natarajan S. *Inorg. Chem. Commun.*, **2004**, **7**:395~399
- [4] Zhang L P, Wan Y H, Jin L P. *Polyhedron*, **2003**,**22**:981~987
- [5] Thirumurugan A, Natarajan S. *Eur. J. Inorg. Chem.*, **2004**: 762~770
- [6] Chui S S Y, Lo S M F, Charmant J P H, et al. *Science*, **1999**, **283**:1148~1150
- [7] Song J L, Ma J G, Sun Y Q, et al. *Eur. J. Inorg. Chem.*, **2003**: 4218~4226
- [8] Wang Y B, Zheng X J, Zhuang W J, et al. *Eur. J. Inorg. Chem.*, **2003**:1355~1360
- [9] Wang Z Q, Kravtsov V C, Zaworotko M J. *Angew. Chem., Int. Ed.*, **2005**,**44**:2~5
- [10] Liu S G, Liu W, Zuo J L, et al. *Inorg. Chem. Commun.*, **2005**, **8**:328~330
- [11] Ye Q, Chen X B, Song Y M, et al. *Inorg. Chim. Acta*, **2005**, **358**:1258~1262
- [12] Huang H M, Wang K M, Tan W H, et al. *Angew. Chem., Int. Ed.*, **2004**,**43**:5635~5638
- [13] Koudoumas E, Konstantaki M, Mavromanolakis A, et al. *Chem. Eur. J.*, **2003**,**9**:1529~1534
- [14] Hou H W, Meng X R, Song Y L, et al. *Inorg. Chem.*, **2002**,**41**: 4068~4075
- [15] Luo J H, Hong M C, Wang R H, et al. *Eur. J. Inorg. Chem.*, **2003**:2705~2710
- [16] Long L S, Chen X M, Tong M L, et al. *J. Chem. Soc., Dalton Trans.*, **2001**:2888~2890
- [17] Zhang X F, Huang D G, Chen C N, et al. *Inorg. Chem. Commun.*, **2005**,**8**:22~26
- [18] Bakalbassis E G, Paschalidis D G. *Inorg. Chem.*, **1998**,**37**: 4735~4737
- [19] Konar S, Manna S C, Zangrando E, et al. *Eur. J. Inorg. Chem.*, **2004**:4202~4208
- [20] Rueff J M, Masciocchi N, Rabu P, et al. *Chem. Eur. J.*, **2002**,**8**:1813~1820
- [21] Rosi N L, Eckert J, Eddaoudi M, et al. *Science*, **2003**,**300**: 1127~1129
- [22] Rowsell J L C, Willward A R, Park K S, et al. *J. Am. Chem. Soc.*, **2004**,**126**:5666~5667
- [23] Dören T, Sarkisov L, Yaghi O M, et al. *Langmuir*, **2004**,**20**: 2683~2689
- [24] Chae H K, Siberio-Pérez D Y, Kim J, et al. *Nature*, **2004**,**427**: 523~527
- [25] Hu M L, Zhu N W, Li X H, et al. *Cryst. Res. Technol.*, **2004**, **39**:505~510
- [26] Sheldrick G M. *Acta Cryst. A*, **1990**,**46**:467~473
- [27] Sheldrick G M. *SHELXL-97, Program for X-ray Crystal Structure Refinement*, University of Göttingen, Germany, **1997**.
- [28] Kissinger H E. *Anal. Chem.*, **1957**,**29**:1702~1706
- [29] Ozawa T. *Bull. Chem. Soc. Jpn.*, **1965**,**38**:1881~1886
- [30] Nyquist R A, Kagel R O. *Infrared Spectra of Inorganic Compounds*. New York: Academic Press, **1971**.220
- [31] MacCallum J R, Tanner J. *Eur. Polymer J.*, **1968**,**4**:333~335
- [32] Satava V, Sestak J. *Thermochim. Acta*, **1975**,**8**:477~489
- [33] Agrawal R K. *J. Therm. Anal.*, **1987**,**32**:149~156
- [34] Achar B N, Brindley G W, Sharp J H. *Proceedings of International Clay Conference, Vol.2*. Israel: Jerusalem, **1966**. 67~69
- [35] Phadnis A B, Deshpande V V. *Thermochim. Acta*, **1983**,**62**: 361~367